Impact Sound Transmission through Floor/Ceiling Systems

Thomas Scelo

Impact Sound Transmission Through Floor/Ceiling Systems

Thomas Scelo
Marshall Day Acoustics, PO Box 5811 Wellesley Street, Auckland 1141, New Zealand
Thomas.scelo@marshallday.co.nz

ABSTRACT
The mechanisms responsible for the transmission of sound in building elements such as floor/ceiling systems are complex and not yet fully understood. In an attempt to understand some of these phenomena, an analytical model was developed for finite and non-periodical floor/ceiling systems to predict their low frequency response to impact excitations. The finite dimensions of the structure are taken into consideration by adopting a modal approach whereby the displacements and pressure fields are expanded into infinite series of admissible functions. The solution relies neither on the periodicity of the stiffened ceiling panels or suspension system nor on the infinite extend of the floor. The paper presents briefly the modelling approach leading to the prediction of the quadratic vibration velocity of the ceiling panel. Finally, comparisons are made between measurements and prediction.

1. INTRODUCTION

Suspended ceilings beneath floors are a very common solution to improve the sound insulation of a floor design. Even though such systems come in a variety of shapes and materials, their geometry seldom deviates greatly from the typical "double-leaf" structure (only ceiling constructions typically used in dwellings are considered here and office type ceiling tiles on channel grids are excluded). Typically, the two "leaves" have the same area, are parallel to each other and are mechanically connected via a suspension system. The ceiling often comprises one or more plasterboard layers. This plasterboard diaphragm is suspended by screws to a grid of parallel ceiling battens which are themselves suspended from the concrete floor. The ceiling cavity is typically filled with a fibrous absorbing material.

The principle of sound transmission through such a system can be separated into three different but inter-dependent paths. A structural path through which vibrations generated in the top plate are transmitted to the lower plate via the suspension system, a fluid path which describes the coupling between the plates due to the compressibility of the fluid in the ceiling cavity and a flanking path through the surrounding structure. This paper does not address the issue of flanking to concentrate on the interactions between the various elements constituting the system.

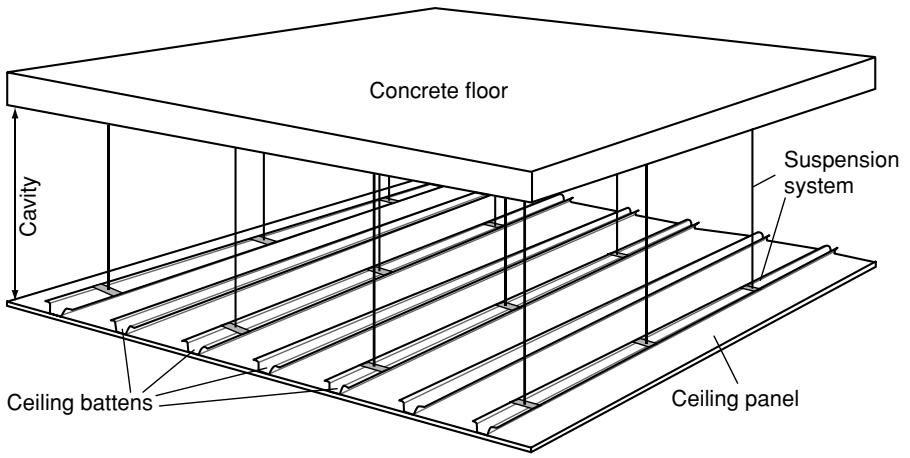

Figure 1. A ceiling suspended from a concrete floor.

A review of the literature [1] has shown that much work, both theoretical and empirical, has been done on the topic especially in the area of lightweight timber floors and monolithic floors. However, it was shown that little is available on the combination of concrete floor and lightweight suspended ceilings. A basic principle has been adopted for both lightweight timber floors [2-5] and concrete floors [6-9] with suspended ceilings whereby the system is conceptualised as a double plate structure. Works treating the problems of double plate structures and ribbed plates are therefore seminal to the study of floor/ceiling sound insulation [10-18]. A closer examination revealed that most previous models relied on the assumption that the framework of ribs is periodic and that the structure is infinite [2, 10, 19-24]. Yet, evidence exists that the response of a finite plate to an impact excitation varies across the plate, depending on how far the excitation and receiver are from the boundary [19, 25-26]. Moreover, a substantial work has been done on disordered periodically ribbed plates [27-38] which provides sufficient clues as to how non-periodic structures can be mathematically handled.

The literature indicates that the prediction of the impact sound insulation of a floor depends on the availability of an accurate model to predict the driving point impedance of the floor [19, 39] which, in turn, needs to be combined with an accurate description of the impact force. Moreover, a substantial amount of data for many types of impact sources is already available [19-20, 38-40]. It can be concluded that there is no urgent need for a new model of impact force for concrete floors.

Other aspects relative to the problem of sound insulation through double leaf structures also need to be considered at low frequencies. In the case of the problem of fluid-structure coupling, it was shown that the coupling between the source and receiving rooms and a modally reactive floor (or wall) has triggered much interest in the acoustic community. Previous studies [41-44], limited to a single leaf panel, have exposed the effects of coupling between the modally reactive rooms and panels. Yet, no theoretical model for

the sound insulation of a double leaf structure between rooms is to be found and only empirical data is available concerning the importance of these effects.

The issue of modelling the infill material in the ceiling cavity has already been addressed extensively leading to sophisticated and very complex prediction models seemingly offering a large choice of approaches [45]. However, as many researchers in building acoustics have concluded, the model for the cavity infill is only considered as a means to include dissipation in the cavity and that the gain in accuracy provided by using complex models such as Biot's [46] or Allard's [47] is not necessarily justified in comparison with the expected accuracy of the model altogether. Such consideration has led many to adopt Delany and Bazley's empirical model [48] or one of its improved versions [49].

The overall conclusion drawn from this literature survey is that although much has been considered regarding the sound and vibration transmission of floor-like structures, little has been done to predict the acoustic performance of suspended ceilings beneath floors. A low frequency model that considers the finite size of the floor, that does not rely on the periodicity of the structure, that includes the fluid loading of the plates from the source and receiving rooms and that predicts the mobility of the system, with an accuracy at least comparable to that of existing models, would constitute a step forward in this already well researched domain.

In this paper, the analytical model used to predict the performances of such a floor/ceiling structure is first presented as a set of equations governing either a vibration displacement field or a sound pressure field of a component of the structure. The solution to this problem is then presented before the numerical predictions are compared with measurement data.

2. ANALYTICAL MODEL

The frequency range considered in this study is 0 to 500 Hz. The displacements and sound pressure fields are written as the sums of trigonometric functions (modeshapes) that describe the vibroacoustic states of each component. The equations governing the dynamic behaviour of these components lead to modal expressions describing the coupling phenomena involved in the structural and fluid transmission paths. These coupling terms between the individual components allow the reduction of the problem to a system of partial differential equations, the unknowns of which are the sets of expansion coefficients for the displacements of the floor and ceiling panel. By writing the problem into a matrix form, the solution is given directly by a single matrix inversion.

2.1. Monolithic floor

The monolithic floor considered in the present study is a single concrete slab of constant thickness h_1, Young's modulus E_1, density ρ_1 and corrected shear modulus G_1^* (Fig. 2). It is modelled as a thick plate with general elastic boundary conditions defined, at each point of the perimeter, by a set of transverse and rotational springs. The ideal boundary conditions (F, SS and C) can then be described by assigning limit stiffness values to the springs. For example, the simply supported edge condition is described by setting the $K^T = 0$ (translation) and rotational $K^R \to \infty$.

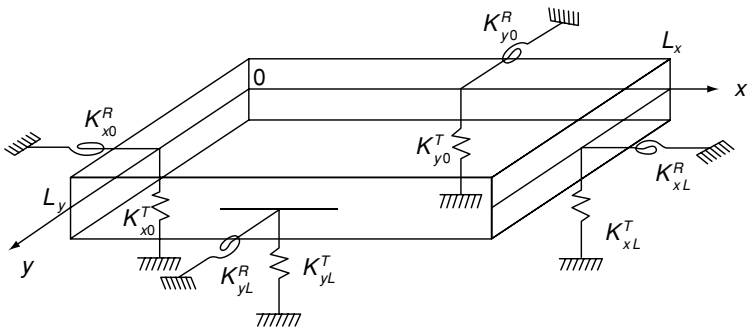

Figure 2. Elastically supported concrete slab.

The boundary conditions are then given by a set of equations accounting for the residual displacements and bending and twisting moments occurring at the edges as a result of the elasticity of the supports. If the transverse displacement of the plate mid-plane is denoted u_1 then one can write

$$\begin{cases} x=0: \quad K^T_{x0}u_1 = Q_x, \quad K^R_{x0}\dfrac{\partial u_1}{\partial x} = -M_{xx}, \\ x=L_x: \quad K^T_{xL}u_1 = -Q_x, \quad K^R_{xL}\dfrac{\partial u_1}{\partial x} = M_{xx}, \\ y=0: \quad K^T_{y0}u_1 = Q_y, \quad K^R_{y0}\dfrac{\partial u_1}{\partial y} = -M_{yy}, \\ y=L_y: \quad K^T_{yL}u_1 = -Q_y, \quad K^R_{yL}\dfrac{\partial u_1}{\partial y} = M_{yy}. \end{cases}$$

where M and Q denote the bending moments and shear forces applied to the plate by the reacting springs. Many functions satisfying the above set of boundary conditions can be considered and in particular trigonometric functions, generated by expanding the displacements into Fourier series. Polynomial functions have also been used, by expanding the displacements into Taylor series [50-52]. The transverse displacement of the concrete floor can then be expanded as

$$u_1(x,y) = \sum_{p,q=1}^{\infty} P_{pq}\Psi_p(x)\Theta_q(y), \tag{1}$$

where P_{pq} are the expansion coefficients (unknowns to the problem). $\psi_p(x)$ and $\Theta_q(y)$ are the modeshapes, each is defined as the sum of the modeshape associated with a simply supported plate and a function of the stiffnesses of the springs at the boundaries [52]. Under a harmonic point excitation force noted F directed normal to the plate, in the positive z-direction, the plate is set in vibration. The transverse displacement field is the solution to the following governing equation

$$\sum_{p,q=1}^{\infty} P_{pq} \iint_S \psi_p^* \Theta_q^* \hat{D}_{pq}^{(1)} \psi_k \Theta_l \, dS = \iint_S \psi_k^* \Theta_l^* \, \hat{N} F \, dS, \tag{2}$$

where $\hat{D}_{pq}^{(1)}$ and $\hat{N} F$ are respectively the operator associated with the governing equation for the transverse displacement of a thick plate and the associated non-homogeneous term [53]. S is the surface area of the concrete floor. For a simply supported plate, the right hand side term of eqn (2) becomes $\hat{D}_{pq}^{(1)} P_{pq} S / 4$ and

$$\hat{D}_{pq}^{(1)} = D_1(\alpha_p^2 + \beta_q^2)^2 - \omega \left[\frac{\rho_1 h_1^3}{12} + \frac{D_1 \rho_1}{G_1^*} \right] (\alpha_p^2 + \beta_q^2) - \rho_1 h_1 \omega^2 \left[1 - \omega^2 \frac{\rho_1 h_1^2}{12 G_1^*} \right], \tag{3}$$

$$\hat{N}F = \left[1 - \frac{D_1 \Delta}{G_1^* h_1} - \omega^2 \frac{\rho_1 h_1^2}{12 G_1^*} \right] F(x,y), \tag{4}$$

where $\alpha_p = p\pi / L_x$, $\beta_q = q\pi / L_y$ and where Δ is the Laplacian operator. The terms introducing the corrected shear modulus G_1^* represent the transverse shear contribution and those containing the ratio $\rho_1 h_1^3 / 12$ the rotary inertia of the plate. Eliminating these terms reduces the equation to that of Kirchhoff's thin plate theory. It is noted that the concrete floor is not only under the point excitation force F but also subjected to the reaction forces from the suspension system attached to it.

2.2. Suspension system

The suspension systems connecting the concrete floor to the ceiling come in a variety of shapes and materials. The concrete floor to rod connection is typically rigid but can also include a damping rubber block. The connection at the other hand consists of a steel clip that can offer both resilience and damping. Additionally, the ceiling batten can contribute significantly to the resilience of the suspension system depending on its shape (Fig. 3). These batten characteristics are here implicitly considered as being part of the suspension system stiffnesses discuss in this section.

The suspension rod is subjected to the forces and moments applied by the vibrating concrete floor and ceiling at its extremities and constitutes a main path of vibration transmission. The forces and moments are expressed at the extremities as functions of the displacement fields u_1 for the concrete floor and u_2 for the ceiling panel.

A wave-based analysis shows that the typical length, stiffnesses and density of such rods result in natural frequencies for longitudinal motion well above the 500 Hz limit. The same analysis shows that one resonance frequency associated with flexural motion falls within the frequency range considered. It is here proposed to use a lumped model approach comprising of longitudinal and flexural springs and dampers where the flexural stiffness is frequency dependent and includes the first flexural resonance frequency of the rod. The combination of above is described by the equivalent dynamic stiffness Z_{eq}. If the suspension system consists of a longitudinal spring K_C, a flexural spring K_M and a damping C_R, then

$$Z_{eq} = K_C + j\omega C_R + K_M \Delta. \tag{5}$$

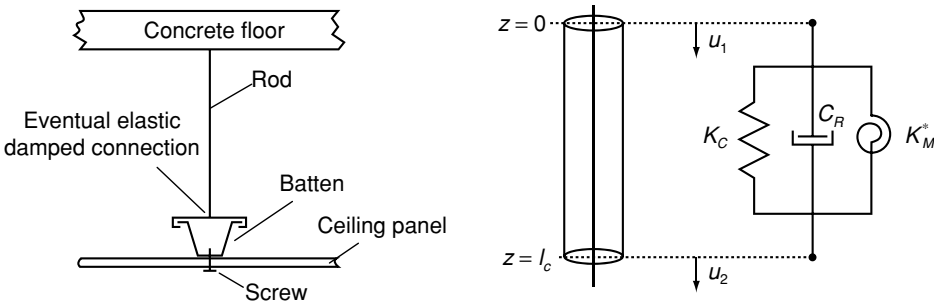

Figure 3. The suspension system and lumped equivalent model

If u_2 denotes the transverse displacement field of the ceiling panel, the reaction force exerted by the suspension system on the concrete floor and suspended ceiling is a function of the transverse displacement difference and angular displacement difference between the two plates:

$$F_{rod} = Z_{eq}\left[u_1(x,y) - u_2(x,y)\right]\delta(x - x_\alpha)\,\delta(y - y_\beta), \tag{6}$$

where (x_α, y_β) denotes the positions of the suspension rod.

2.3. Ceiling panel

Ceiling panels generally consist of a single or double layer of gypsum board, stiffened by an array of ceiling battens and are, typically, supported by peripheral "L-shaped" channels (Fig. 4). The array of battens is, in most cases, periodic. The model proposed here does not assume any periodicity in the battens' and rods' distributions so that the performances of a wider range of designs can be predicted. Series of simple vibration level measurements on battens and peripheral channels [1] have shown that the boundary conditions of the ceiling battens and ceiling panel, when screwed to the peripheral channel, can be modelled with reasonable accuracy as simply supported, allowing for rotation but no transverse displacements.

Typically, ceiling panels are periodically screwed to the array of battens. Experience [1, 54] has shown that these screw connections are best modelled as rigid point connections when the bending wavelength in the panel is shorter than five times the screw spacing and as a rigid line connection otherwise. Each batten is modelled as a beam under multiple driving point forces, located at the connections with the suspension rods, and set in bending and torsional motion. The ceiling diaphragm is modelled as a single thin classical plate as the length and width of ceilings far exceed the thickness of the plasterboard.

Considering that all battens are parallel to each others, the locations of the battens can then be fully defined by a finite set of coordinates the dimension of which is equal to the number of battens in the system. If one assumes that the screws are aligned along each batten, the locations of the connections between battens and ceiling panels are fully defined by the coordinates of each screw.

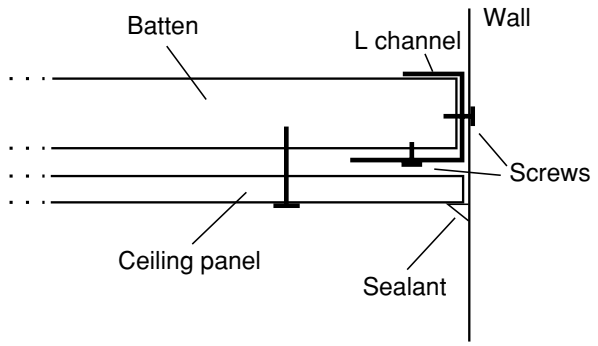

Figure 4. Boundary conditions for ceiling panel and battens.

The reaction force exerted by the battens on the ceiling panel can then be written as

$$F_{bat} = \hat{H}\, u_2(x,y)\,\delta(x-x_b)\;\delta\;(y-y_s \text{ with}$$

$$\hat{H} = EI_y \frac{\partial^4}{\partial y^4} + GJ_y \frac{\partial^4}{\partial x^2 \partial y^2} - \omega^2 \rho_b \left(S_b - I_p \frac{\partial^2}{\partial x^2} \right), \tag{7}$$

where EI_y and GJ_y are respectively the complex flexural and torsional stiffnesses, ρ_b is the density, S_b the cross-sectional area and I_P the polar moment of inertia of the battens; (x_b, y_s) are the coordinates of the screws.

If the displacement field of the ribbed ceiling panel is decomposed in a basis of eigenfunctions $\phi_p(x)\zeta_q(y)$ satisfying the boundary conditions above, and if the expansion coefficients are denoted C_{pq} so that

$$u_2(x,y) = \sum_{p,q=1}^{\infty} C_{pq} \phi_p(x) \zeta_q(x), \tag{8}$$

the equation governing the displacement field can be written as

$$\hat{D}_{pq}^{(2)} C_{pq}\,(S/4) = \sum_{\alpha,\beta} \iint_S F_{bat}\, \phi_p \zeta_q dS + \sum_{r,s} \iint_S F_{rod}\, \phi_p \zeta_q dS, \tag{9}$$

where $\hat{D}_{pq}^{(2)} = \overline{D}_2(\alpha_p^2 + \beta_q^2)^2 - \rho_2 h_2 \omega^2$.

Note that the classical plate theory is used for the ceiling plasterboard panels.

2.4. Cavity

Typically, the cavity is partly filled with a fibrous material for attenuation of the sound transmission from the floor to the ceiling panel via the air in the cavity. The partly filled cavity is modelled as two subsequent media of propagation (Fig. 5). The vertical walls of the cavity are assumed impervious.

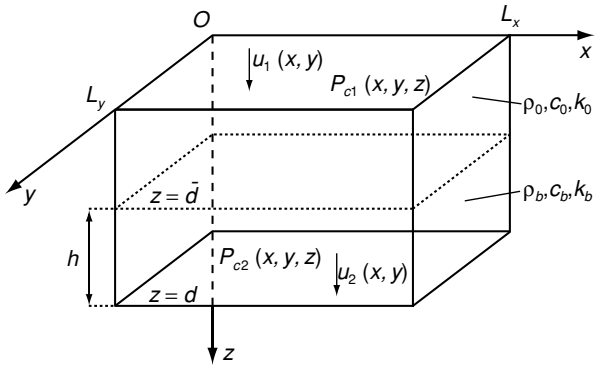

Figure 5. Cavity with infill, notations.

The first domain of propagation is defined by $0 \le z \le \bar{d}$ and the medium of propagation is air (characteristic impedance $\rho_0 c_0$, wavenumber $k_0 = \omega / c_0$). The second domain of propagation is defined by $\bar{d} \le 0 \le d$ and the medium of propagation is modelled as an equivalent dissipative fluid with the complex characteristic impedance Z_{fib} defined in [48] as a function of the airflow resistivity σ of the fibrous material [49]. The complex impedance results in a complex propagation constant k_{fib}. The two Helmholtz equations governing the sound pressure field in the sub-domains are respectively written as

$$[\Delta + k_0^2\ ]\, p_{C1}(x,y,z) = 0, \quad \forall\, z \in [0, \bar{d}\,], \tag{10}$$

$$[\Delta + k_{fib}^2]\, p_{C2}(x,y,z) = 0, \quad \forall\, z \in [\bar{d}, d]. \tag{11}$$

The conditions of continuity of the acoustic and mechanical velocities at the solid-fluid ($z = 0$) and fluid-solid ($z = d$) interfaces leads to relationships between the sound pressure fields in the cavity and the displacements u_1 and u_2 of the plates:

$$\left.\frac{\partial p_{C1}}{\partial z}\right|_{z=0} = \omega^2 \rho_0 u_1 \text{ and } \left.\frac{\partial p_{C2}}{\partial z}\right|_{z=d} = \omega^2 \rho_{fib} u_2. \tag{12}$$

Finally, the continuity of the particle velocity at the interface between the two media of propagation gives a direct relationship between the sound pressure fields [55]

$$\left.\frac{\partial p_{C2}}{\partial z}\right|_{z=\bar{d}} = \frac{\rho_{fib}}{\rho_0} \left.\frac{\partial p_{C1}}{\partial z}\right|_{z=\bar{d}} \tag{13}$$

The sound pressure field is written as the summation over the acoustic modeshapes of the cavity, given as $\Phi_p(x)\Omega_q(y) = \cos[p\pi x / L_x]\cos[q\pi y / L_y]$, so that

$$p_{C1}(x,y,z) = \sum_{p,q} \xi_{pq}(z)\Phi_p(x)\Omega_q(y), \tag{14}$$

$$p_{C2}(x,y,z) = \sum_{p,q} \lambda_{pq}(z)\Phi_p(x)\Omega_q(y), \tag{15}$$

the substitution of eqns (14-15) into eqns (10-13) leads directly to the expressions for the sound pressure fields as functions of the expansion coefficients P_{pq} and C_{pq} of the plates' displacements.

2.5. Source and receiving rooms

In practice, the floors considered are always separating two rooms of finite dimensions. The outgoing acoustic waves generated by the vibrating ceiling panel do meet boundaries and are partly reflected back toward the ceiling. Stationary waves may build up and the effect of the fluid loading is then a combination of mass, stiffness (due to the compressibility of the air) and resonant behaviour. The effects of backing cavities on the dynamic response and radiation of flexural panels have been investigated using various approaches such as finite elements [44] or modal analysis [41-43]. It was shown that the sound level difference between two rooms separated by a given structure (floor or wall) is not only a characteristic of the structure but also of its environment, comprising the junctions, the source room and the receiving room.

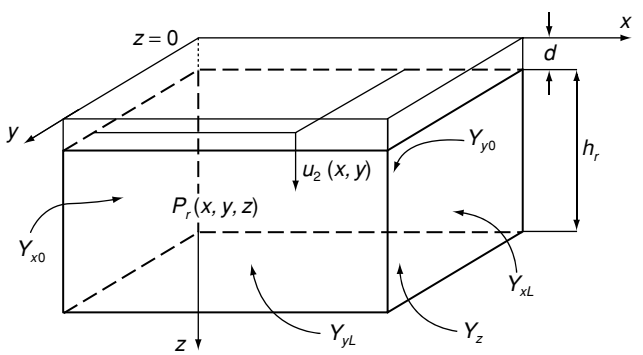

Figure 6. Notations associated with the receiving room and vibrating ceiling panel at $x = d$.

The following approach is detailed for the receiving room coupling with the vibrating ceiling panel. However, the same steps can be followed to treat the problem of coupling between the source room and the concrete floor. The boundaries of the room (walls and floor) are represented by their characteristic admittances Y.

If $p_R(x,y,z)$ denotes the sound pressure at any given point (x,y,z) in the room, then Helmholtz equation can be written as

$$(\Delta + k_0^2) p_R(x,y,z) = 0, \quad \forall x \in [0, L_x], \forall y \in [0, L_y], \forall z \in [d, d + h_r]. \tag{16}$$

The sound pressure field that is the solution to the above problem must also satisfy the boundary conditions imposed by the energy dissipative walls and floor:

$$\begin{aligned} &\left.\frac{\partial p_R}{\partial x}\right|_{x=0} = jk_0 Y_{x0} p_R, \quad \left.\frac{\partial p_R}{\partial y}\right|_{y=0} = jk_0 Y_{y0} p_R, \quad \left.\frac{\partial p_R}{\partial z}\right|_{z=d} = \omega^2 \rho_0 u_2(x,y), \\ &\left.\frac{\partial p_R}{\partial x}\right|_{x=L_x} = -jk_0 Y_{xL} p_R, \quad \left.\frac{\partial p_R}{\partial y}\right|_{y=L_y} = -jk_0 Y_{y0} p_R, \quad \left.\frac{\partial p_R}{\partial z}\right|_{z=d+h_r} = -jk_0 Y_z p_R. \end{aligned} \tag{17}$$

In this investigation, the values of the admittances at the boundaries are assumed equal for opposite walls so that $Y_{x0} = Y_{xL} = Y_x, Y_{y0} = Y_{yL} = Y_y$. The solution to the above problem is sought as a series of admissible functions satisfying the boundary conditions (17). The variations of the pressure field in the z-direction are included in the associated expansion coefficients $\Lambda_{pq}(z)$:

$$p_R(x,y,z) = \sum_{p,q=1}^{\infty} \Lambda_{pq}(z) \tilde{\Omega}_p(x) \tilde{\Xi}_q(y). \tag{18}$$

The admissible functions that satisfy the boundary conditions are given in ref. [55] as

$$\Omega_p(x)\Xi_q(y) = \cos\left(k_p x - jY_x \frac{k_0}{k_p}\right) \cos\left(\kappa_q y - jY_y \frac{k_0}{\kappa_q}\right), \tag{19}$$

where (δ denoting the Kronecker delta)

$$\begin{cases} \tilde{k}_p = \left(\dfrac{p\pi}{L_x}\right)^2 + j(2-\delta_{p0}) 2\dfrac{k_0}{L_x} Y_x, \\ \tilde{\kappa}_q = \left(\dfrac{q\pi}{L_y}\right)^2 + j(2-\delta_{q0}) 2\dfrac{k_0}{L_y} Y_y. \end{cases} \tag{20}$$

Substituting eqns (18-20) into eqn (16) leads to the determination of the coefficients $\Lambda_{pq}(z)$ as sums of waves propagating in the z-direction and depending on the boundary conditions along the two other. Substituting the result into eqns (17) provides the expressions for the magnitudes of these waves as functions of the expansions coefficients associated with the displacement field of the ceiling panel. Similarly, the same approach for the source room leads to the expression of the sound pressure field in the source $p_S(x,y,z)$ as function of the expansion coefficients associated with the displacement of the concrete floor.

2.6. Solution

The problem can now be fully defined by writing the equations governing the displacements of the floor and ceiling panel as

$$\begin{cases} \sum_{p,q=1}^{\infty} \hat{D}_{pq}^{(1)} P_{pq} \Psi_p(x)\Theta_q(y) = F_e \delta(x-x_e)\delta(y-y_e) - \sum_{\alpha,\beta=1}^{Nrod} \boldsymbol{F}_{rod} - p_{C1}(x,y,0) + p_S(x,y,0) \\ \sum_{p,q=1}^{\infty} \hat{D}_{pq}^{(2)} C_{pq} \phi_p(x)\zeta_q(y) = \sum_{\alpha,\beta=1}^{Nrod} F_{rod} - \sum_{r,s=1}^{Nscrew} F_{bat} + p_{C2}(x,y,d) - p_R(x,y,d). \end{cases}$$

harmonic point force excitation; reaction forces from suspension system (eqs. 5 - 6); reaction from the ceiling cavity (eq. 14); fluid loading from source room

mass, stiffness, shear and rotatory inertia of concrete slab (eqs. 1 - 4)

mass and stiffness of ceiling panel (eqs. 8 - 9); excitation from suspension system; reaction from ceiling battens (eq. 7); reaction from the ceiling cavity (eq. 15); fluid loading from receiver room (eqs. 18 - 20)

(21)

Multiplying the first equation of the system (21) by the modeshape $\Psi_k(x)\Theta_l(y)$ and the second equation by $\phi_k(x)\zeta_l(y)$ and integrating over the surface areas of the floor defined by $S = \{0 \le x \le L_x, 0 \le y \le L_y\}$, before applying the orthogonality relationships between modeshapes leads to a new system of equations which, when written in a matrix form, becomes

$$\begin{aligned} \left[\Lambda D^{(1)} + 4\Lambda\Theta + P_{C1/1} - P_S\right]\{P\} + \left[-4\Lambda\Theta + P_{C1/2}\right]\{C\} &= 4\Lambda[B], \\ -\left[4\Lambda\Theta + P_{C2/1}\right]\{P\} + \left[\Lambda D^{(2)} + 4\Lambda\Theta + H - P_{C2/2} + P_R\right]\{C\} &= 0, \end{aligned} \tag{22}$$

where $D^{(1)}$ and $D^{(2)}$ denote respectively the sums of the stiffness and inertia matrices associated with the free vibrations of the uncoupled floor and ceiling panel; Θ is the matrix associated with the finite sum of all local forces and moments applied by the rods, H denotes the matrix associated with the reaction force from the battens to the displacement of the ceiling panel, $P_{Ci/j}$ are the matrices of modal coupling terms between the ith part of the cavity on the jth plate and $[B]$ is the coupling matrix between the driving point force and the modal displacement of the floor. $\{P\}$ and $\{C\}$ are vectors, the components of which are respectively the expansion coefficients P_{pq} and C_{pq}. Finally, condensing the system of matrix eqns (17) into a single equation

$$\begin{bmatrix} [\Lambda D^{(1)} + 4\Lambda\Theta + P_{C1/1} - P_S] & [-4\Lambda\Theta + P_{C1/2}] \\ -[4\Lambda\Theta + P_{C2/1}] & [\Lambda D^{(2)} + 4\Lambda\Theta + H - P_{C2/2} + P_R] \end{bmatrix} \begin{bmatrix} \{P\} \\ \{C\} \end{bmatrix} = \begin{bmatrix} 4\Lambda[B] \\ 0 \end{bmatrix} \tag{23}$$

leads, after inversion of eqn (18), to the expression of the expansion coefficients C_{pq} for the displacement of the ceiling panel. The vibration velocity of the ceiling panel is then directly reconstructed using eqn (8). The mean-square vibration velocity of the ceiling panel is directly available for a given harmonic point excitation force applied to the concrete floor [10].

Figure 7. Array of battens suspended from a concrete floor before the installation of the ceiling panel.

3. NUMERICAL RESULTS

3.1. Experimental data

The system considered is shown in Fig. 7, consisting of a 140 mm concrete slab to which were rigidly connected an array of fifteen 180 mm long steel rods. Five parallel battens were suspended from the array of rods, 600 mm apart, before a sheet of 13 mm gypsum was screwed to the battens. The screws were set at 200 mm centres.

The characteristics of the materials used for the measurement and simulations are given in Table 1. The same values were used for the prediction of the mobility.

The harmonic point force was provided by a B&K4809 electromagnetic shaker driven with a random signal generated by a HP3566A dynamic signal analyser, amplified by a Ling TPO25 amplifer and mounted onto a rigid frame above the concrete slab. A PCB208C02 force transducer measured the excitation signal (Fig. 8).

Two PCB352C68 accelerometers with PCB480E09 power supplies were used to measure the vibration acceleration of the suspended ceiling from which the transfer mobility of the whole system was derived. The acceleration signal was recorded over a period of 1 second and the averaged spectrum of the signal averaged over 128 repetitions of the measurement at 37 different positions over the surface area of the ceiling.

The point and space-averaged mobilities of the system were derived from the acceleration signal. The space-averaged mobility is defined as equal to the normalised quadratic velocity of the ceiling panel, was estimated as

$$< H > = \frac{1}{|F|} \left[\frac{1}{S} \iint_S (j\omega u_2)^* (j\omega u_2) dS \right]^{1/2} \tag{24}$$

Table 1: Characteristics of the materials

Concrete		**Ceiling**	
E_1 (Nm^{-2})	$29\ 10^9$	E_2 (Nm^{-2})	$2.8\ 10^9$
h_1 (mm)	140	h_2(mm)	13
ρ_1 (Kgm^{-3})	2400	ρ_2 (Kgm^{-3})	700
Rods		**Battens**	
E_c (Nm^{-2})	$210\ 10^9$	E_y (Nm^{-2})	$210\ 10^9$
ρ_c (Kgm^{-3})	7500	I_y (m^4)	11.910^{-9}
length(mm)	180	Jy(m^4)	510^{-12}
radius(mm)	6	ρ_b(Kg m^{-3})	7500
		S_b(m^2)	6610^{-6}
Cavity		**Dimensions of system**	
σ(mksRayls/m)	4135	L_x(m)	3.4
d(mm)	180	L_y(m)	3.4
$\bar{d}$(mm)	105		

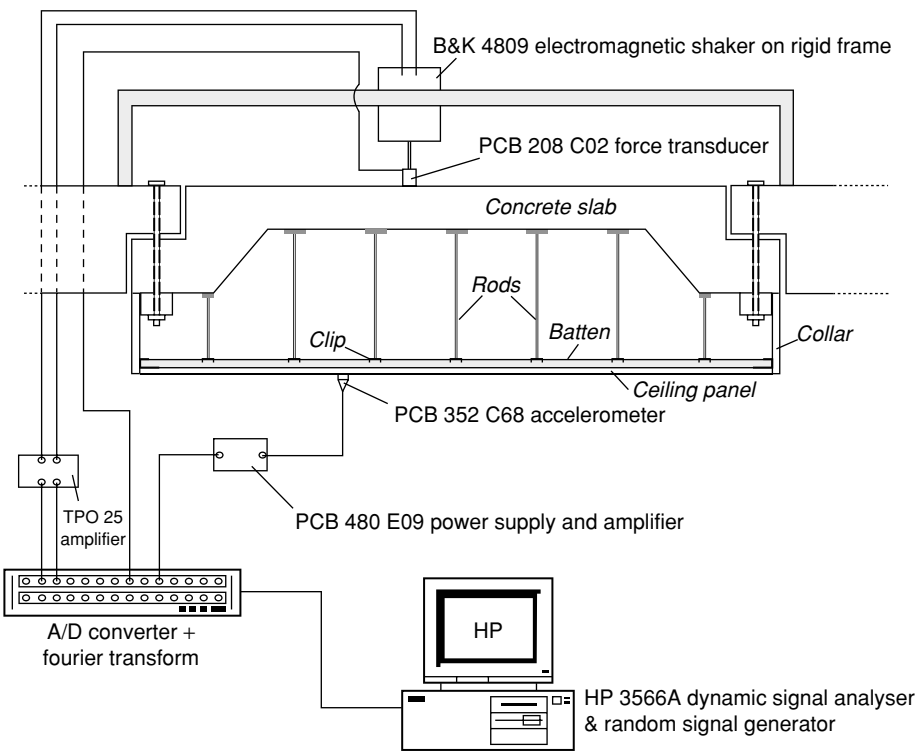

Figure 8. Experimental setup.

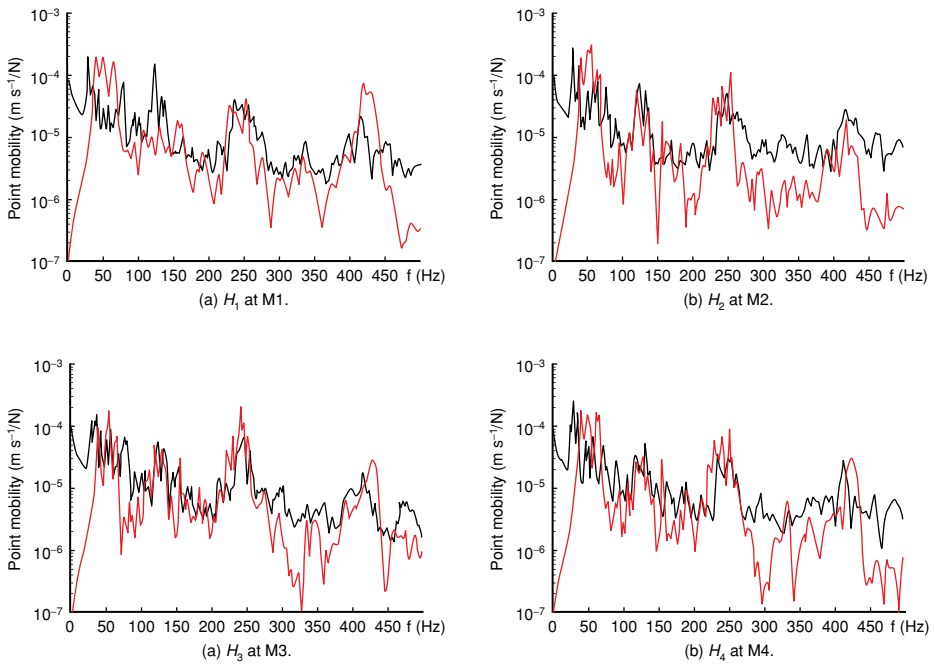

Figure 9. Measured (—) and predicted (—) point mobilities of the suspended ceiling for four different excitation and measurement point.

where * is the complex conjugate.

The predicted and measured space-averaged mobilities are shown in Figs. 9 and 10 for comparison.

Fig. 9 shows that the predicted point mobilities are in relatively good agreement with the measured point mobility. The region in the very low frequencies (f < 50 Hz) cannot be accurately predicted due to the elastic boundary conditions of the concrete floor used for the measurement. However, for frequencies above this limit, the predicted mobility exhibits similar frequency content to that of the measured mobility. The differences between the predicted and measured point mobilities are, for some frequencies, more than one order of magnitude.

The predicted space averaged mobilities shown in Fig. 10, calculated while assuming the concrete slab simply supported above 50 Hz and elastically supported below 50 Hz, are compared to the measured space averaged mobility. The space averaged mobility is calculated over the entire set of measurement points while the predicted mobility is calculated by averaging over the entire surface area of the suspended ceiling.

Fig. 10 shows that the predicted and measured space averaged mobilities of the suspended ceiling are in reasonably good agreement for frequencies above 50 Hz. It can

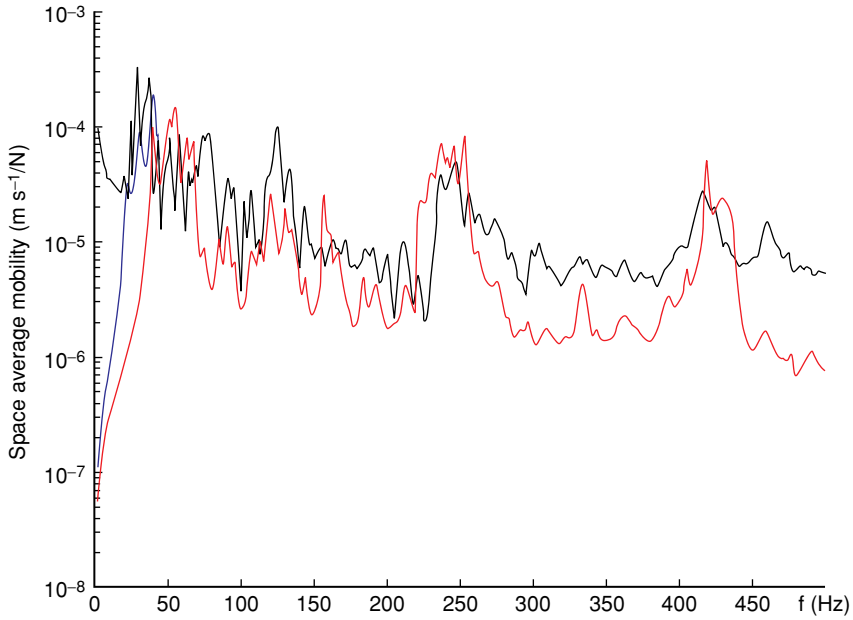

Figure 10. Measured (—) and predicted averaged mobilities of the suspended ceiling: (—): simply supported concrete slab across the frequency range, (—): elastically supported slab below 50 Hz.

be seen that the resonance frequencies of the concrete floor influence significantly the mobility of the entire system. The locations of the resonance peaks around 112 Hz, 250 Hz and 430 Hz are well predicted. However, the limited number of modes in the prediction results in a drop of the agreement between the predicted and measured space averaged mobilities above 440 Hz. It can be seen that the model does well in predicting the main trends of the response, especially the dominance of the resonance frequencies of the concrete floor. The model, however, under-estimates the response of the system which, one could expect, might result from errors in assigning material properties and thus render the coupling terms weaker than they actually are. Indeed, experience tells us that some material characteristics and some aspects of the system's geometry can significantly affect the magnitude and frequency content of the space averaged mobility. Fig. 11 gives the level difference between the measured and predicted mobility (i.e. twenty times the logarithm (base 10) of the ratio of the measured space averaged mobility to the predicted space averaged mobility).

The mean value of the relative difference calculated over the entire spectrum considered is equal to 9.0 dB when the concrete slab is simply supported and to 7.1 dB when it is considered elastically supported below 50 Hz. The dynamic range of the relative differences spreads over 40 dB and the local maximum deviations occur around the resonance frequencies of the concrete floor at 224 Hz and 430 Hz.

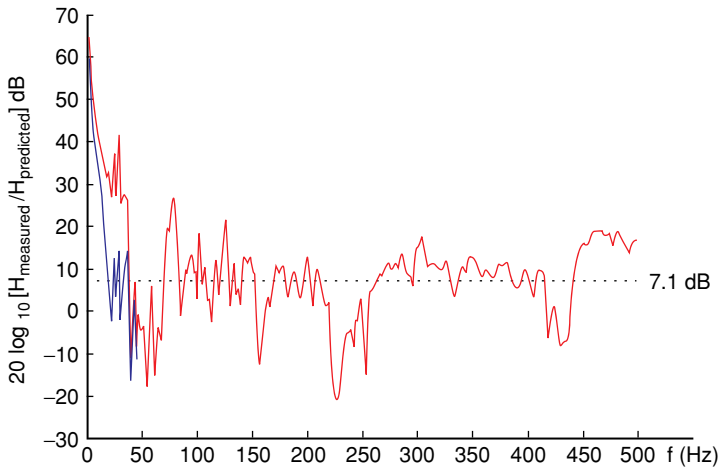

Figure 11. Relative difference between measured and predicted mobilities. (—): simply supported concrete slab across the frequency range, (—): elastically supported slab below 50 Hz.

There are many possible reasons to explain the lack of detailed agreement between the measured and predicted responses of the system. First, the boundary conditions of the real concrete slab are difficult to estimate. The present model can only assume simply supported or homogeneous and frequency independent elastic boundary conditions. The concrete slab used for the measurement was in fact bolted up (8 bolts along the perimeter) to the surrounding floor. Secondly, the boundary conditions of the cavity and ceiling panel are only approximate ones while in practice; there will always be a fraction of energy dissipated within the vertical walls of the cavity and the peripheral channels. Thirdly, the damping in all structural components of the structure is introduced as a constant loss factor when it is, in reality, a frequency dependent quantity which needs to be measured for all modes within the frequency range considered. Finally, the material properties can only be estimated and they are assumed identical for all battens, all plasterboard sheets and all suspension rods. In reality, these characteristics exhibit a degree of variability. The effect of such variability can if fact be investigated using the present model as the latter does not rely on a strict periodicity of geometry or material properties.

The agreement at low frequencies ($f < 350$ Hz) between the measured and predicted point and space averaged mobilities would certainly improve if the properties of all the components used during the experimental campaign had been experimentally determined. It can however be concluded that the model predicts reasonably well the response of the system to a point force applied onto the concrete floor.

4. CONCLUSION

In this paper, a model for predicting the dynamic response of a suspended ceiling beneath a floor was briefly presented. Limiting the analysis to the low frequency range, the modal

decomposition of the displacement fields and sound pressure fields offers the benefit of isolating the different coupling terms between the different elements of the system.

The problem is simplified by combining the equations governing the displacement fields of the concrete floor and ceiling panel and that governing the sound pressure field in the cavity into a single matrix equation that can be numerically solved with a single matrix inversion.

It was shown that such a model can predict the dynamic response of a suspended ceiling beneath a floor with reasonable accuracy while offering a realistic approach by considering the finite size of the system, the elastic boundary conditions of the concrete floor, the partial filling of the cavity and the non-periodicity of the battens' and rods' distributions.

ACKNOWLEDGMENTS

The author would like to thank Dr. C.R. Halkyard and Dr. G. Dodd from the University of Auckland for their comments and guidance. This work was funded by the Foundation for Research Science and Technology (contract WSWL301).

REFERENCE

[1] Scelo T., *Sound transmission through concrete floors and suspended ceiling systems – a vibroacoustic analysis*, PhD Thesis, University of Auckland, 2006.

[2] Brunskog J., *Acoustics excitation and transmission of lightweight structures*, Technical report, Engineering Acoustics, LTH TVBA-1009, 2002.

[3] Chung H., Introduction to a fourier series solution method to vibrations of joist floors, in *Proceedings of the 17th Biennial Conference of the New Zealand Acoustical Society*, Wellington, 2004, 7–12.

[4] Chung H. *et al*., *Maximising impact sound resistance of timber framed floor/ceiling systems*, Technical report, FWPRDC Project PN04, 2006.

[5] Emms G. *et al*., Improving the impact insulation of light timber floors, in *Proceeding of Wespac IX*, Seoul, 2006, volume Paper No212.

[6] Rindel J. H., *Sound insulation course*, New Zealand Acoustical Society, Auckland, 2002.

[7] Patrício J. V., *Comportamento Acústico de Pavimentos Não-Homogenéneos de Edifícios A Sons de Impacto*, PhD thesis, Technical University of Lisboa, 1998.

[8] Gerretsen E., Calculation of the sound transmission between dwellings by partitions and flanking structures, *Applied Acoustics*, 1979, 12, 413–433.

[9] Gerretsen E. Calculation of airborne and impact sound insulation between dwellings, *Applied Acoustics*, 1986, 19, 245–264.

[10] Cremer L. *et al*., *Structure-borne Sound,* 2nd Edition, Springer-Verlag, Berlin, 1973.

[11] Berry A., *Vibrations et Rayonnement acoustique de structures planes complexes immergées dans un fluid léger ou dans un fluid lourd,* PhD thesis, Université de Sherbrooke, 1991.

[12] Snowdon J. C., Vibration of simply supported rectangular and square plates to which lumped masses and dynamic vibration absorbers are attached, *Journal of the Acoustical Society of America,* 1975, 57(3), 646–654.

[13] Rumerman M. L., Vibration and wave propagation in ribbed plates, *Journal of the Acoustical Society of America*, 1975, 57, 370–373.

[14] Mace B., The vibration of plates on two-dimensionally periodic point supports, *Journal of Sound and Vibration*, 1996, 192(3), 629–643.

[15] Mace B., Sound radiation from a plate reinforced by two sets of parallel stiffeners, *Journal of Sound and Vibration*, 1980, 71(3), 435–441.

[16] Mace B., Periodically stiffened fluid-loaded plates, i: response to convected harmonic pressure and free wave propagation, *Journal of Sound and Vibration*, 1980, 73(4), 473–486.

[17] Mace B., Periodically stiffened fluid-loaded plates, ii: response to line and point forces, *Journal of Sound and Vibration*, 1980, 73(4), 487–504.

[18] Mace B., Sound radiation from fluid loaded orthogonally stiffened plates, *Journal of Sound and Vibration*, 1981, 79(3), 439–452.

[19] Kimura S. & Inoue K., Practical calculation of floor impact sound by impedance method, *Applied Acoustics*, 1989, 26, 263–292.

[20] Vér I. L., Impact noise isolation of composite floors *Journal of the Acoustical Society of America*, 1971, 50(4), 1043–1050.

[21] Lindblad S., *Impact sound characteristics of resilient floors coverings: a study on linear and nonlinear dissipative compliance*, PhD thesis, Division of Building Technology, Lund Institut of Technology, Lund, Sweden, 1968 (as reported in ref. [2]).

[22] Takahashi D., Sound radiation from periodically connected double-plate structures, *Journal of Sound and Vibration*, 1983, 90, 541–557.

[23] Skelton E., Acoustic scattering by parallel plates with a single connector, *Proceedings of the Royal Society of London A*, 1990, 427, 401–418.

[24] Skelton E., Acoustic scattering by parallel plates with periodic connectors. *Proceedings of the Royal Society of London A*, 1990, 427, 419–444.

[25] Rindel J. H., Dispersion and absorption of structure-borne sound in acoustically thick plates, *Applied Acoustics*, 1994, 41, 97–111.

[26] Emms G., Predicting footstep noise using tapping machine measurements of floor impact insulation, in *Proceedings of the 16th Biennial Conference of the New Zealand Acoustical Society*, Auckland 2002, 11–21.

[27] Mace B. *et al*., Preface: Uncertainty in structural dynamics, *Journal of Sound and Vibration*, 2005, 288, 423–429.

[28] Anderson P. W., Absence of diffusion in certain random lattices, *Physics Review*, 1958, 09(5), 1492–1505.

[29] Hodges C. H., Confinement of vibration by structural irregularity, *Journal of Sound and Vibration*, 1982, 82(3), 411–424.

[30] Hodges C. H. & Woodhouse J., Vibration isolation from irregularity in a nearly periodic structure: theory and measurements, *Journal of the Acoustical Society of America*, 1983, 74(3), 894–905.

[31] Pierre C. *et al*., Localized vibrations of disordered multispan beams: theory and experiment, *AAIA*, 1987, 25(9), 1249–1257.

[32] Pierre C. & Cha P. D., Strong mode localization in nearly periodic disordered structures, *AAIA*, 1989, 27(2), 227–241.

[33] Boyce W.E., A "dishonest" approach to certain stochastic eigenvalue problem, *SIAM Journal of Applied Mathematics*, 1967, 15, 143–152.

[34] Cai G. Q. & Lin Y. K., Statistical distribution of frequency responses in disordered periodic structures, *AIAA*, 1992, 30(5), 1400–1407.

[35] Langley R. S., Wave transmission through one-dimensional near periodic structures: optimum and random disorder, *Journal of Sound and Vibration*, 1995, 188(5), 717–743.

[36] Bansal A. S., Free waves in periodically disordered systems: natural and bounding frequencies of unsymmetric systems and normal mode localization, *Journal of Sound and Vibration*, 1997, 207(3), 365–382.

[37] Ibrahim R. A., Structural dynamics with parameter uncertainties, *Applied Mechanics Review*, 1987, 40(3), 309–328.

[38] Coyette J. P., Sources of uncertainties in vibro-acoustic simulations, *Acoustique & Techniques*, 2005, 40(1), 26–32.

[39] Shi W. *et al*., *An investigation of the characteristics of impact sound sources - Tulea 1995:06*, Technical report, Lulea University of Technology, Sweden, 1995.

[38] JIS A 1418, *Method for field measurement of floor impact sound level*, Japanese Standards, 1978.

[39] Patrício J. V. & Martins de Silve P., *The importance of concrete elastic characteristics variations on the structure-borne sound insulation index*., Technical report, Memória No 819, Laboratório Nacional de Engenharia Civil, Lisboa, Portugal, 1999.

[40] Harris C. M., *Harris' shock and vibration handbook*, McGraw-Hill, New York, 2002.

[41] Dowell E. H. & Voss H.M., The effect of a cavity on panel vibration, *AAIA*, 1962, 1(2), 476–477.

[42] Pretlove A. J., Forced vibrations of a rectangular panel backed by a closed rectangular cavity, *Journal of Sound and Vibration*, 1966, 3(3), 252–261.

[43] Guy R. W., The response of a cavity backed panel to external airborne excitation: a general analysis, *Journal of the Acoustical Society of America*, 1979, 65(3), 719–731.

[44] Maluksi S. & Gibbs B. M., The effect of construction material, contents and room geometry on the sound field in dwellings at low frequencies, *Applied Acoustics*, 2004, 65, 31–44.

[45] Attenborough K., Acoustical characteristics of porous materials, *Phys. Reports Rev. Sect. Phys. Letters*, 1982, 82(3), 179–227.

[46] Biot M. A., Theory of propagation of elastic waves in a fluid-saturated porous solid, *Journal of the Acoustical Society of America*, 1956, 28, 168–191.

[47] Allard J.-F., *Propagation of sound in porous media*, Elsevier Applied Science, 1993.

[48] Delany M. E. & Bazley E. N., Acoustical properties of fibrous absorbent materials, *Applied Acoustics*, 1970, 3, 105–116.

[49] Voronina N., Improved empirical model of sound propagation through a fibrous material, *Applied Acoustics*, 1996, 48, 121–132.

[50] Li W. L., Free vibrations of beams with general boundary conditions, *Journal of Sound and Vibration*, 2000, 237,709–725.

[51] Li W. L., Dynamic analysis of beams with arbitrary elastic supports at both ends, *Journal of Sound and Vibration*, 2001, 246(4), 751–756.

[52] Li W. L., An analytical solution for the self- and mutual-radiation resistances of a rectangular plate, *Journal of Sound and Vibration*, 2001, 245(1), 1–16.

[53] Skudrzyk E., *Simple and complex vibratory systems*, The Pennsylvania State University Press, London, 1968.

[54] Craik R. J. M. & Smith R. S., Sound transmission through double leaf lightweight partitions part 1: airborne sound, *Applied Acoustics*, 2000, 61, 223–245.

[55] Bruneau M. & Scelo T., *Fundamental Acoustics*, ISTE, London, 2006.